VII International Conference on Particle-Based Methods
PARTICLES 2021
P. Wriggers, M. Bischoff, E. Oñate, A. Düster & T. Zohdi (Eds)

A HYBRID TIME-FREQUENCY METHODOLOGICAL PROPOSAL TO SIMULATE GROUND RESPONSE UNDER HARMONIC ACCELERATIONS IN A MATERIAL-POINT FRAMEWORK

Cristian D. Rodríguez[1,2], **Luis F. Prada-Sarmiento**[2a], **Torsten Wichtmann**[2b]

[1] Bauhaus-Universität Weimar
Coudraystraße 11c, 99423 Weimar, Germany
e-mail: cristian.rodriguez@uni-weimar.de

[2] Ruhr-Universität Bochum
Gebäude IC Etage 5, 44801 Bochum, Germany
[a] e-mail: luis.pradasarmiento@rub.de
[b] e-mail: torsten.wichtmann@rub.de

Key words: Material point method, Fourier analysis, Seismic ground response, MPM-FEM coupling

Abstract. The response of geomaterials to seismic excitations, which are usually described with time history data, can be estimated by solving governing equations in the frequency domain and transferring quantities back to the time domain. However, one limitation of frequency analysis is the simplification of soil response by assuming constant stiffness during the action of seismic input. Therefore, when the frequency approach is used in ground response problems, linear-equivalent models of soil behaviour that allow the description of non-linear stiffness are implemented. In order to simulate large fields of displacements induced by seismic actions, this paper introduces a methodological proposal based upon a hybrid Finite Element (FE) time-frequency approach, coupled with the Material Point Method (MPM). In the FE solution, the soil stiffness changes after certain number of cycles and the equation of motion is solved in the frequency domain while the soil stiffness remains constant. Mapping of kinematic quantities between nodes of the finite element mesh and material points is performed via a Newton-Raphson numerical scheme. Each change of the stiffness matrix is marked by a convective material-point phase and the recalculation of material point locations. By following this approach, large deformations of geomaterials under constant amplitude harmonic accelerations can be simulated using a linear equivalent approach for the non-linear response. A model test case subjected to harmonic shaking is explained.

1 INTRODUCTION

Background Earthquake-induced movements might cause significant damages in buildings and infrastructure. The propagation of earthquakes across soil deposits can amplify the waves on the ground surface. Amplified waves can produce the collapse of buildings or trigger landslides on natural or artificial slopes. In particular, worst-case scenarios of earthquake-induced landslides involve large deformations of soils or rocks, affecting human settlements, infrastructure, the environment, or the natural habitat of animal species. In this context, the estimation of the runout of earthquake-induced landslides is of interest to geotechnical engineers for risk assessment. The extension and reach of a landslide depends, amongst other factors, on the failure mechanism that governs the instability of the soils under driving actions. Landslides often involve interactions between the sliding mass, the sliding surface, the compressibility of the geomaterials, loss of shear strength, capillarity, and changes in the pore water pressures of the soil mass.

Hence the importance of a good an accurate prognosis of the seismic ground response. Besides, there are other less critical scenarios that involve large deformations of soils; for example, soil penetration and controlled explosions. The failure mechanism and progression of landslides and other large deformation problems in different scenarios can be predicted by means of numerical simulations. Such simulations require a framework that accounts for large deformations of solids, make use of complex constitutive models with plenty of parameters to be determined from in-situ and laboratory tests, and are usually performed incrementally by solving equations of motion in time domain due to the nonlinear nature of the geomaterials under consideration.

Problem statement In this paper a framework for the solution of seismic ground response of geomaterials under ideally drained conditions subjected to harmonic accelerations is presented. In particular, cyclic behaviour of soils is considered by adopting linear-equivalent characteristics of soil behaviour. The material point method (MPM) is used to take into account the large deformation process ensuing the failure and post-failure phases. The framework is valid for a three dimensional mass of soil although first attempts are simulated under plane strain conditions. In this paper a solution to the equations of motion in the frequency domain for different lapses of time of the acceleration time history is proposed. Such accelerations represent a seismic action on the ground. Continuity of the response is ensured by convective MPM phases between signal lapses.

Notation In this paper matrices and tensors are denoted with capital bold letters (e.g. $\mathbf{M}$, $\mathbf{K}$, $\boldsymbol{\sigma}$, $\mathbf{J}$), vectors are denoted with lower-case bold letters (e.g. $\mathbf{u}$, $\ddot{\mathbf{u}}$, $\mathbf{h}$, $\mathbf{r}$) and $\mathbb{1}$ is a column vector of ones. Scalars, functions and other variables are denoted in lowercase or capital letters without bold (e.g. $\ddot{u}_b(t)$, X_i, Y_i).

2 STATE OF THE ART

MPM was first proposed by Sulsky et al. [1], [2] as an extension of the existing particle-in-cell method for fluids to simulate solids. The main advantages of the MPM are its fully Lagrangian framework and the weak formulation of the method being consistent with that of the finite element method (FEM). MPM was initially proposed in an explicit formulation to solve transient problems for solids; additionally, implicit schemes have also been proposed in the literature [3], [4], [5]. Bardenhagen et al. [6] proposed an application of MPM for discrete media considering grain compressibility.

Extensions of the MPM for geomaterials include hydro-mechanical coupling [7], [8], [9], [10], [11], [12], [13], [14], [15], granular column collapse [16], penetration problems [17], [18], random fields in combination with MPM for simulation of retrogressive behaviour of landslides [19] and soil dynamics [8], [20], [21]. MPM simulations of real case studies of landslides have been conducted by Zabala and Alonso [22], Yerro [10] and Liu et al. [23].

3 THEORETICAL FRAMEWORK

The solution of governing equations and the hybrid time-frequency approach for geomaterials is introduced and discussed in this section.

3.1 Governing equations

Equation of motion Following Bathe (2014) the updated Lagrangian (UL) finite element formulation of the equation of motion for dynamic analysis with implicit time integration is [24]:

$$\mathbf{M}\ddot{\mathbf{u}} + \mathbf{K}^{*}\mathbf{u} = -\mathbf{f} \tag{1}$$

Where $\mathbf{K}^{*}$ is the complex stiffness matrix, $\mathbf{K}^{*} = \mathbf{K} + i\omega\mathbf{C}$, $\mathbf{M}$ is the consistent mass matrix, $\ddot{\mathbf{u}}$ is the nodal acceleration vector, $\mathbf{u}$ is the increment of the nodal displacement vector and $\mathbf{f}$ is the nodal point inertial force vector. In the seismic case the inertial force vector is expressed as:

$$\mathbf{f} = \mathbf{M}\,\mathbb{1}\,\ddot{u}_b(t) \tag{2}$$

Where $\ddot{u}_b(t)$ is the seismic acceleration signal at the base of the numerical model.

Determination of matrices The stiffness matrix is calculated as:

$$\begin{aligned} \mathbf{K} &= \mathbf{K}_L + \mathbf{K}_{NL} \\ \mathbf{K}_L &= \int_V \mathbf{B}_L^\top \, \mathbf{D} \, \mathbf{B}_L \, dV \\ \mathbf{K}_{NL} &= \int_V \mathbf{B}_{NL}^\top \, \boldsymbol{\sigma} \, \mathbf{B}_{NL} \, dV \end{aligned} \tag{3}$$

Where $\mathbf{K}_L$ is the linear strain incremental stiffness matrix, $\mathbf{K}_{NL}$ is the nonlinear strain (geometric or initial stress) incremental stiffness matrix, $\mathbf{B}_L$ is the linear strain displacement transformation matrix, $\mathbf{B}_{NL}$ is the non-linear strain displacement transformation matrix, $\mathbf{D}$ is the linear elastic stress-strain material matrix and $\boldsymbol{\sigma}$ is the Cauchy stress tensor.

The consistent nodal mass matrix is calculated based on Sulsky [1]:

$$\mathbf{M} = \mathbf{S}^\top \mathbf{M}_p \mathbf{S} \tag{4}$$

Where $\mathbf{S}$ is the mapping matrix evaluating shape functions at material points and $\mathbf{M}_p$ is the lumped mass matrix with material point masses.

3.2 Solution in the frequency domain

Equation (1) can be solved in the frequency domain following the equivalent linear approach of seismic ground response for dynamic finite element analysis stated by Kramer (1996) [25]. Considering seismic harmonic accelerations, the relative displacement vector can be calculated as:

$$\mathbf{u} = \mathbf{h}(\omega)\widehat{\ddot{u}_b}(\omega)e^{i\omega t} \tag{5}$$

Where $\widehat{\ddot{u}_b}(\omega)$ is the Fourier transform of $\ddot{u}_b(t)$ and $\mathbf{h}(\omega)$ is a vector of spectral functions in the frequency domain, so-called transfer functions.

Transfer functions Transfer functions link the response at nodal values of a finite element model with the input signal, in this case with $\widehat{\ddot{u}_b}(\omega)$. The solution of Equation (1) requires an intermediate step in which the vector $\mathbf{h}(\omega)$ is determined based on the consistent mass matrix and the complex stiffness matrix:

$$\mathbf{h}(\omega) = [\omega^2 \mathbf{M} - \mathbf{K}^*]^{-1} \mathbf{M} \, \mathbb{1} \tag{6}$$

3.3 Hybrid time-frequency approach

The disadvantage of a solution of the type shown in the previous section lies on the limitation of a solution by means of Fourier analysis, which is the consideration

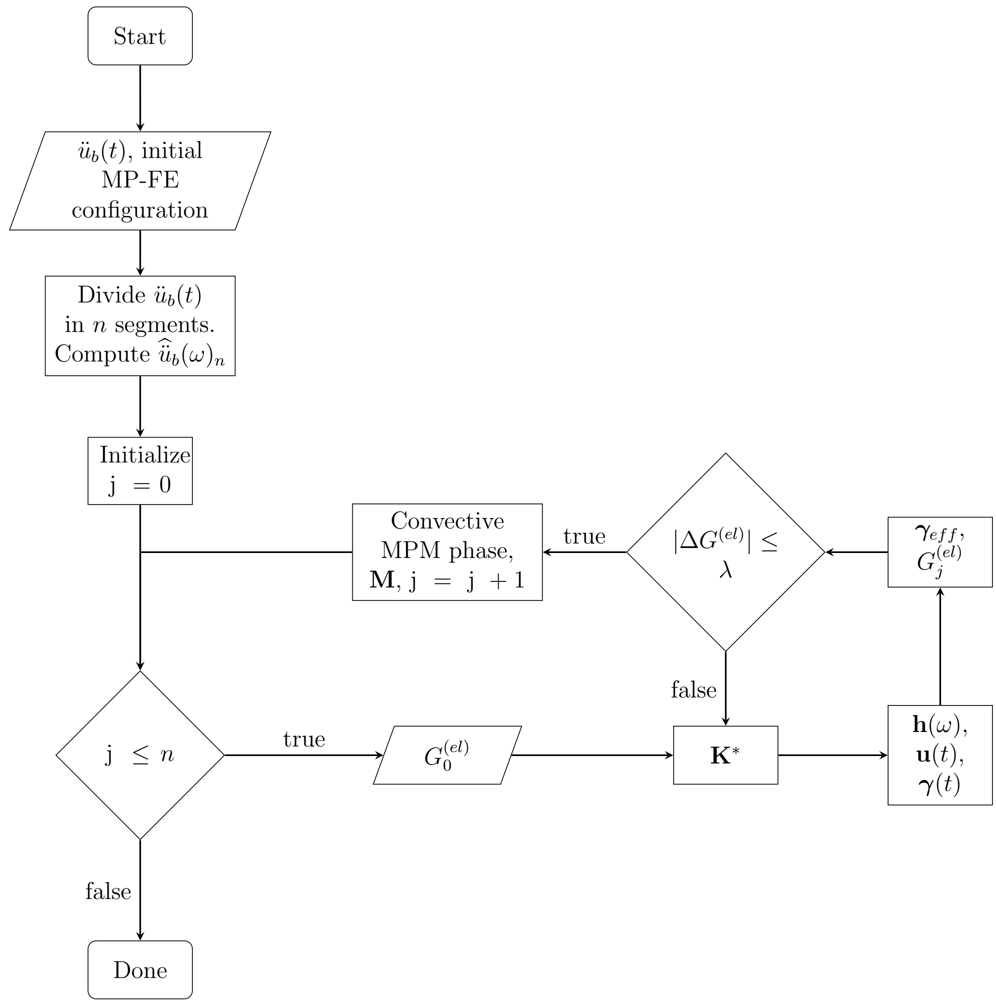

Figure 1: Flow chart of the hybrid time-frequency approach for linear-equivalent response of soils

of constant stiffness over-time. In order to consider seismic ground response via Fourier analysis, the following approach is suggested:

Divide the seismic signal $\ddot{u}_b(t)$ in a n number of lapses with the same Δt. Thus, stiffness and mass matrices change n times during the simulation. Calculate the functions $\widehat{\ddot{u}_b}(\omega)_j$ for j between 1 and n and build the initial consistent mass matrix. For each lapse between 1 and n: Assume an initial shear modulus of the soil at element level $G_0^{(el)}$ and determine the complex stiffness matrix of the current grid-material point set. Compute the vector $\mathbf{h}(\omega)_j$ and the response of the system in terms of nodal displacements relative to the base excitation, Equation (5), in accordance with the UL formulation presented above. This step requires the estimation of corresponding values of shear modulus per element based on an iterative scheme where a tolerance value λ must be larger than the magnitude between two consequtive values of shear modules per element. Therefore, the element stiffness matrices will change from those calculated with $G_0^{(el)}$; at the end of each lapse, each element is associated to an updated value of shear modulus $G_j^{(el)}$. Afterwards, map new locations of material points based on nodal relative displacements by means of MPM interpolation, so-called convective phase, and determine a new consistent mass matrix for the next lapse.

The above mentioned approach is assumed to overcome the problems of large deformations associated with conventional finite-elements for the simulation of seismic-induced landslides. Figure 1 illustrates the procedure explained in this section with a flowchart.

Inverse material point - finite element mapping The evaluation of finite element shape functions at material points in this work is done by following a Newton-Raphson numerical scheme in order to find the natural coordinates of a material point located within a finite element. The problem involves the calculation of the roots of non-linear equations in two dimensions.

Finite element mapping is conventionally performed from known natural coordinates of points lying within an element to global coordinates of a finite element configuration. Inverse mapping is less trivial because it involves the solution of a set of non-linear equations, as many equations as dimensions considered in the geometry, to find the natural coordinates of material points within finite elements. In Figure 2 an example of conventional and inverse mapping for a particle within a four-noded finite element is presented.

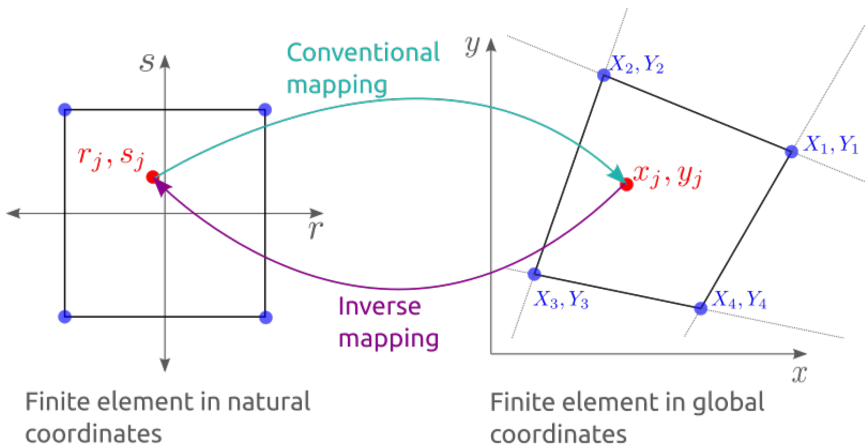

Figure 2: Mapping locations between natural and global coordinates of particles within a four-noded finite element

For a two-dimensional configuration, natural coordinates r and s must be determined. Inverse mapping via a Newton-Raphson scheme requires to find values of residual functions $g(r,s)$ that approach zero (see Equation (7)).

$$\begin{aligned} g_1(r,s) &= \sum_i N_i(r,s)\cdot X_i \ - x \\ g_2(r,s) &= \sum_i N_i(r,s)\cdot Y_i \ - y \end{aligned} \tag{7}$$

Where N_i are finite element shape functions, X_i and Y_i are the nodal coordinates of the finite element configuration and x, y are the coordinates of a material point. The roots of g_1 and g_2 are determined numerically by assuming an initial vector of local coordinates $\mathbf{r_j}$ and iteratively solving Equation (8) for $\mathbf{r_{j+1}}$.

$$\mathbf{r_{j+1}} - \mathbf{r_j} \ = \ -\mathbf{J_j}\ \mathbf{g_j} \tag{8}$$

Where $\mathbf{J_j}$ is the Jacobian matrix of the residual functions evaluated at $\mathbf{r_j}$.

$$\mathbf{J_j} \ = \ \begin{bmatrix} \dfrac{\partial g_1(r_j,s_j)}{\partial r} & \dfrac{\partial g_2(r_j,s_j)}{\partial r} \\ \dfrac{\partial g_1(r_j,s_j)}{\partial s} & \dfrac{\partial g_2(r_j,s_j)}{\partial s} \end{bmatrix} \tag{9}$$

4 NUMERICAL EXAMPLE

An elastic column subjected to vertical accelerations at nodal points is simulated using the approach described above. The inner loop of Figure 1 accounting for the linear-equivalent behaviour typical of soils is not yet incorporated in the present results and two materials are chosen in order to test the method on a configuration with multiple materials. Thus, only linear elastic parameters are chosen for the upper and lower sections of the column. The column has a height of 100 meters and a width of 4 meters. The geometry is divided into 20 plane strain elements with a height of 5 meters and 4 material points per cell are originally located within each element (see Figure 3). The parameters of the 2 material sets are shown in Table 1.

The acceleration signal imposed to the column is $\ddot{u}_b(t)$[m/s^2]$=\sin\left(\dfrac{2\pi}{100}t\right)$. The calculation undergoes one cycle of the outer most for loop shown in Figure 1. Thus,

Table 1: Parameters of the elastic column

Material set	E [MPa]	ν	ϱ [kg/m^3]
1	2000000	0.3	7800
2	4.432	0.3	1560

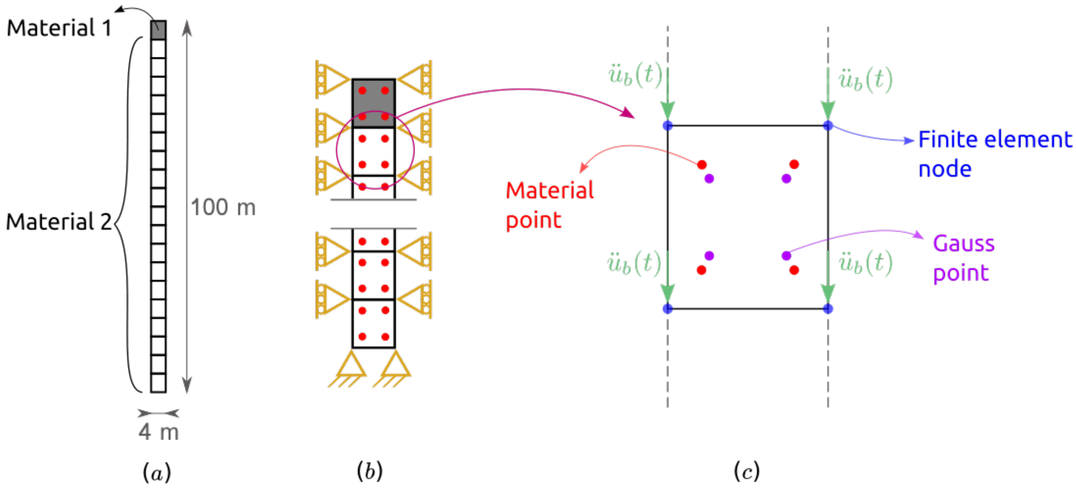

Figure 3: Elastic soil column problem definition in a MPM framework: model dimensions (a), boundary conditions and material points per cell (b) and external accelerations imposed at a finite element level (c).

transfer functions are evaluated, displacement time histories of the finite element nodes are determined and mapped to the material points via the aforementioned inverse mapping procedure. Relative displacements of three nodes of the finite element mesh and three material points are shown in Figure 4.

Node n1 and material point mp1 experience almost zero relative displacements due to the high value of stiffness of the material at the top of the column. Node n2 and material point mp2 reach a relative displacement amplitude of almost 0.7 mm. Amplitude of relative displacements decrease from the interface between the two materials to the base of the column.

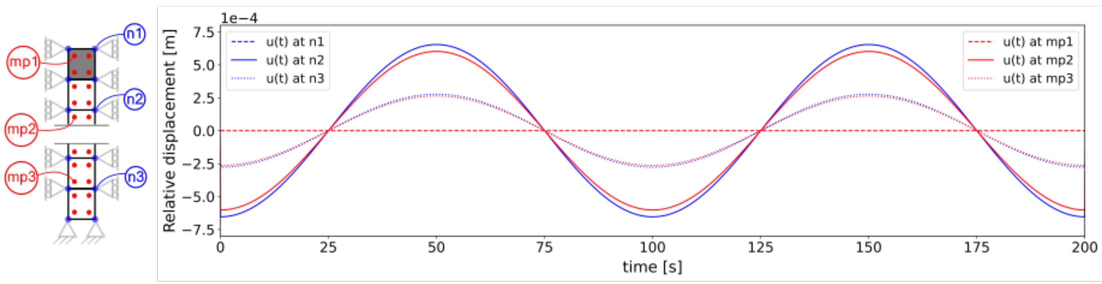

Figure 4: Relative displacements of the column subjected to a harmonic acceleration, three nodes of the finite element grid and three material points are shown.

5 CONCLUSIONS AND FUTURE WORK

A framework to calculate the linear-equivalent seismic response of geomaterials using the material point method has been introduced by discussing theoretical aspects of a hybrid time-frequency methodological proposal. The authors proposed to solve governing equations in the frequency domain for segments of a time history of nodal accelerations. Afterwards, kinematic quantities are transferred back to the time domain in order to perform convective phases between finite element nodes and material points. The method is expected to take into account large deformations of soils subjected to seismic scenarios.

As a limitation of the method, the formulation summarized in section 3.2 would only be valid for constrained degrees of freedom in the perpendicular direction of base excitation in the plane strain case. The formulation must be revised to consider more general cases of two and three dimensional cyclic deformations of soils. A numerical scheme based on Newton-Raphson method was used to map material points to the natural coordinates of a finite element. Inverse mapping equations for a material point within a plane strain finite element were presented and they can be applied to any two-dimensional problem with higher-order elements. The numerical scheme could be easily extended to the three-dimensional case.

Additionally, a numerical example in which an elastic column was excited vertically while constrained horizontally was shown. The convective phase between finite element nodes and material points was effectively achieved in the example. The recalculation of displacements of material points belongs to the last process of the outer most loop of the proposed hybrid time-frequency method. Numerical implementation of Equation (6) for the problem of the elastic column showed that transfer functions reached small absolute values. Thus, calculated relative displacements are small when compared to the total displacements of the system subjected to nodal accelerations.

Finally, the authors expect to simulate the linear-equivalent response of the column shown in the example considering non-linear properties of real soils in order to use all features of the hybrid time-frequency method for a relatively trivial case. Earthquake-induced landslides and other problems involving large deformations of soils considering cyclic shear modulus degradation could be simulated following the proposed methodology. The technique must be compared to other well-known solutions for transient response of geomaterials and more examples will contribute to the validation of the method.

REFERENCES

[1] Sulsky, D., Chen, Z., Schreyer, H.L., 1994. A particle method for history-dependent materials. Computer Methods in Applied Mechanics and Engineering 118, 179–196.

[2] Sulsky, D., Zhou, S.-J., Schreyer, H.L., 1995. Application of a particle-in-cell method to solid mechanics. Computer Physics Communications 87, 236–252.

[3] Guilkey, J.E., Weiss, J.A., 2003. Implicit time integration for the material point method: Quantitative and algorithmic comparisons with the finite element method. Int. J. Numer. Meth. Engng. 57, 1323–1338.

[4] Sulsky, D., Kaul, A., 2004. Implicit dynamics in the material-point method. Computer Methods in Applied Mechanics and Engineering 193, 1137–1170.

[5] Wang, B., Vardon, P.J., Hicks, M.A., Chen, Z., 2016. Development of an implicit material point method for geotechnical applications. Computers and Geotechnics 71, 159–167.

[6] Bardenhagen, S.G., Brackbill, J.U., Sulsky, D., 2000. The material-point method for granular materials. Computer Methods in Applied Mechanics and Engineering 187, 529–541.

[7] Yerro, A., 2011. Solving hydro-mechanical problems with the material point method, in: Proceedings of the 21st European Young Geotechnical Engineers' Conference. pp. 318–323.

[8] Jassim, I., Stolle, D., Vermeer, P., 2013. Two-phase dynamic analysis by material point method: MATERIAL POINT METHOD, TWO-PHASE ANALYSIS, LOW-ORDER ELEMENT. Int. J. Numer. Anal. Meth. Geomech. 37, 2502–2522.

[9] Abe, K., Soga, K., Bandara, S., 2014. Material Point Method for Coupled Hydromechanical Problems. J. Geotech. Geoenviron. Eng. 140, 04013033.

[10] Yerro, A., 2015. MPM modelling of landslides in brittle and unsaturated soils.

[11] Yerro, A., Alonso, E., Pinyol, N., 2016. Modelling large deformation problems in unsaturated soils. E3S Web Conf. 9, 08019.

[12] Bandara, S., Soga, K., 2015. Coupling of soil deformation and pore fluid flow using material point method. Computers and Geotechnics 63, 199–214.

[13] Liang, D., Zhao, X., Martinelli, M., 2017. MPM Simulations of the Interaction Between Water Jet and Soil Bed. Procedia Engineering 175, 242–249.

[14] Liang, D., Zhao, X., Soga, K., 2020. Simulation of overtopping and seepage induced dike failure using two-point MPM. Soils and Foundations 60, 978–988.

[15] Yamaguchi, Y., Takase, S., Moriguchi, S., Terada, K., 2020. Solid–liquid coupled material point method for simulation of ground collapse with fluidization. Comp. Part. Mech. 7, 209–223.

[16] Ceccato, F., Leonardi, A., Girardi, V., Simonini, P., Pirulli, M., 2020. Numerical and experimental investigation of saturated granular column collapse in air. Soils and Foundations 60, 683–696.

[17] Ceccato, F., Beuth, L., Vermeer, P.A., Simonini, P., 2016. Two-phase Material Point Method applied to the study of cone penetration. Computers and Geotechnics 80, 440–452.

[18] Ceccato, F., Beuth, L., Simonini, P., 2016. Analysis of Piezocone Penetration under Different Drainage Conditions with the Two-Phase Material Point Method. J. Geotech. Geoenviron. Eng. 142, 04016066.

[19] Wang, B., Vardon, P.J., Hicks, M.A., 2017. The Random Material Point Method, in: Geo-Risk 2017. Presented at the Geo-Risk 2017, American Society of Civil Engineers, Denver, Colorado, pp. 460–466.

[20] Bhandari, T., Hamad, F., Moormann, C., Sharma, K.G., Westrich, B., 2016. Numerical modelling of seismic slope failure using MPM. Computers and Geotechnics 75, 126–134.

[21] Ceccato, F., Yerro, A., Girardi, V., Simonini, P., 2021. Two-phase dynamic MPM formulation for unsaturated soil. Computers and Geotechnics 129, 103876.

[22] Zabala, F., Alonso, E.E., 2011. Progressive failure of Aznalcóllar dam using the material point method. Géotechnique 61, 795–808.

[23] Liu, X., Wang, Y., Li, D.-Q., 2020. Numerical simulation of the 1995 rainfall-induced Fei Tsui Road landslide in Hong Kong: new insights from hydro-mechanically coupled material point method. Landslides 17, 2755–2775.

[24] Bathe, K.-J., 2014. Finite element procedures, 2nd ed. Ed. Prentice-Hall, Englewood Cliffs, N.J.

[25] Kramer, S., 1996. Geotechnical Earthquake Engineering. Prentice-Hall International Series.